Finite Element Analysis of the O-ring Behavior Under Uniform Squeeze Levels and Internal Pressure

E. EL BAHLOUL[1], H. AISSAOUI[1], M. DIANY [2], E. BOUDAIA [2], S. TOUAIRI[2]

[1]Automation and Energy Conversion Team, Faculty of Science and Technology, Sultan Moulay Sliman University, Beni Mellal, MOROCCO

[2]Industrial Engineering Laboratory, Faculty of Science and Technology, Sultan Moulay Sliman University, Beni Mellal, MOROCCO

Abstract: - The variety of applications, in all industrial fields, whether for routine use or a specific application, requires the design of increasingly efficient sealing systems. O-rings are fundamental elements in many industrial devices and machines, thanks to advantages such as low cost, small size, cleanliness, and ease of assembly. Moreover, the O-ring is available in thousands of dimensions.

In this work, the analysis of the mechanical and leakage behavior of the O-ring seal, when installed either in a groove or between two plates, is presented.

The behavior of the assemblies in both scenarios when the clamping force and fluid pressure are applied is investigated using two numerical models generated with Ansys software.

The numerical model findings are compared to the analytical approach based on Hertz contact theory and other researchers' experimental results. This study shows that the use of a groove to ensure the mounting of elastomeric O-rings is important in pressurized installations. Furthermore, for different pressure conditions, the reliability of the O-ring strongly depends on three parameters: compression ratio of the seal, the hardness of the seal, and the friction coefficient.

Keywords: - O-ring, groove, analytical model, finite element model, contact pressure, fluid pressure

Received: December 23, 2021. Revised: November 6, 2022. Accepted: December 4, 2022. Published: December 31, 2022.

1. Introduction

The modern industry nowadays handles a lot of polluting, toxic, radiative, and flammable products which require more precise knowledge of the sealing function to avoid any possible leakage of these dangerous products. In practice, commercial O-rings are designed to increase contact pressure as the fluid pressure increases. They also require a secure seal, as well as economical manufacturing and easy assembly. Due to its symmetrical shape and inexpensive production cost, the O-ring may appear to be an easy-to-use and effective seal at first glance.

When consulting patent databases, it is only in the 1930s that the term "O-ring" appears. The O-ring was invented by Niels Christensen to seal a piston/cylinder application [1]. Lindley [2] points out the lack of scientific results that would allow a better understanding of the functioning of O-rings. And indeed, research on O-rings did not begin until a few years after these. The equations developed until today to analytically determine the distribution of the contact pressure against the joint-structure contact surfaces are deduced from the classical Hertzian contact theory [3]. Less attention was paid to O-rings inserted in grooves until 1988 when Dragoni et al. [4] studied the mechanical behavior of a non-pressurized O-ring installed in a rectangular groove. The seal in this study is modeled by a flat disk and is subjected to an axial deformation due to the clamping force. This concept was subjected to numerical, experimental, and analytical analysis. Karaszkiewicz [5] has just completed and enriched these previous models, with an analytical model allowing determining the geometrical distortion, the width, and the contact pressure of an O-ring subjected to radial compression and installed in a rectangular groove.

This model enables for the fluid pressure exerted to the joint to be taken into account. The numerical results of George [6] have supported the findings of this study. However, the equations proposed in this model have an error of up to 30% which explains the difficulty of modeling the mechanical behavior of O-rings in pressurized installations. Eshel [7] uses an experimental setup to predict the fluid pressures that cause O-ring extrusion to determine the parameters of his analytical model. Also, as a function of service pressures and the hardness of the rubber utilized, establish the limitations of mechanical extrusion clearance.

In 1998, Yokoyama et al. [8] experimentally determined the change in contact pressure as a function of change in fluid pressure for an O-ring installed in an axial assembly. The seals used were Polyacrylate (ACM), Fluorocarbon (FKM) propylene (EPDM) with different hardnesses. The results obtained show that the lower the hardness of the seal, the

higher the rate of change of the contact pressure at the seal-structure contact surfaces as a function of the fluid pressure. Other experimental works [9], [10], [11] have obtained a satisfactory agreement with the theoretical results. They proposed a photoelasticity-inspired test method. They devised the method to investigate the contact pressure distribution and internal stresses of an O-ring in a rectangular groove. Other researchers [12], [13] will focus on the effect of the friction coefficient on O-ring sealing performance.

In assemblies with O-rings, finite element analysis is present in the majority of published works. This approach has been used on a variety of seals in the literature, including rectangular seals [14], [15], U-shaped seals [16], [17], and O-rings [18], [19]. Using the same method Diany et al. [20] [21] developed a finite element model to study the short-term relaxation of a non-pressurized O-ring. This study showed the effect of the groove in reducing the initial crush required to create the contact pressure that can ensure sealing. El Bahloul et al. [22] have shown that one of the main parameters in the evaluation of O-rings installed in a groove is undoubtedly the contact pressure distribution between the seal and the contact surfaces and that the proper functioning of the O-ring depends on the best choice of the values of the extrusion clearance and the coefficient of friction in pressurized installations. In other works [23], [24], the same authors studied the effect of the groove shape and the effect of introducing a metal core inside the elastomer O-ring. The results of the first study showed that the use of a concave groove, or rectangular groove link, produces more contact pressure and thus further limits the risk of leakage. The second study showed that the introduction of a metal core inside the elastomeric O-ring can improve not only the strength of the seal but also the maximum value of the contact pressure.

O-rings are fundamental elements in many industrial devices and machines, thanks to advantages such as low cost, small size, cleanliness, and ease of assembly. In addition, the O-ring is available in thousands of sizes. However, seal failure due to incorrect mounting conditions, wrong choice of O-ring material, or O-ring geometry leads to lower system performance. Conversely, a better knowledge of the characteristics of the O-ring and its support will improve the performance and efficiency of the systems being sealed. It will prolong the seal's life, allowing it to be employed in a variety of industrial applications. In this work, finite element models, using Ansys software [25], are proposed to evaluate the behavior of the O-ring assembly subjected to combined loads: clamping force and fluid pressure.

2. Modeling of the Studied Assemblies

Large elastic deformations and quasi-incompressible behavior are required when modeling the mechanical behavior of elastomers. Thus, mechanical behavior laws must be formulated in the context of large deformation modeling [26],[27],[28]. The behavior laws most commonly used by commercial calculation software are Mooney Rivlin, Ogden, and Neo Hook. The so-called hyperelastic model of Mooney Rivlin [29] is the most commonly encountered model for describing the mechanical behavior of elastomers. This one allows describing correctly the behavior of an elastomer up to a strain level of 200 % [30].

Knowing all the geometrical parameters as well as the behavior law of the seal material, the positioning of the O-ring can be simulated. The elements of the assembly are simulated in their operating position taking into account the geometrical conditions of the ISO 3601 standard [31]. Figure 1 shows the studied assemblies. Table I lists the mechanical and geometrical features of the assemblies. The joint is modeled by a disk with 2D planar elements with four nodes (PLANE182). Contact elements, CONTA171 and TARGE169, are used to simulate the reaction between the elements that are in contact. Figure 2 shows an example of the O-ring mesh.

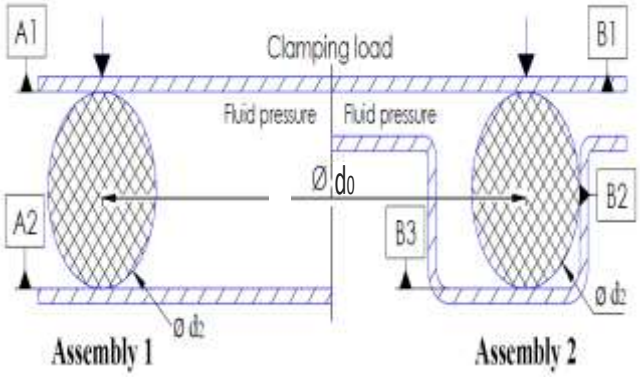

Figure 1 - O-ring assembly between two plates (Assembly 1), O-ring assembly in a groove (Assembly 2)

Table I - Mechanical and geometrical characteristics of the assemblies

Symbol	Designation	Contact
B1	Top surface	O-ring - groove
B2	Lateral surface	
B3	Lower surface	
A1	Top surface	O-ring-plates
A2	Lower surface	
		Values
d_0	O-ring inner diameter	16.35 mm
d_2	O-ring cross-section diameter	2.65 mm
E_1	Young's modulus of the O-ring	13.8 MPa

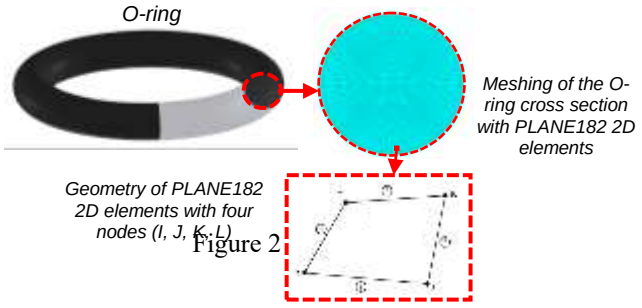

Figure 2

The simulation of the joint assemblies was performed in two steps. In the first step, the joint is compressed between a plate and a groove (Figure 3 (b)) or between two plates (Figure 4 (b)) under the assumption of large deformations and large displacements. The plates and grooves were defined as rigid analytical elements. The displacements of the inner plate in assembly 1 and the groove in assembly 2 were canceled in all directions. The top plate in both assemblies, whose displacements are canceled in the radial direction, is axially loaded by a uniformly distributed clamping force. In the second step, fluid pressure is applied to the active side of the joint (Figure 3 (c) and Figure 4 (c)) for all surface elements that are not in contact with the groove and plates.

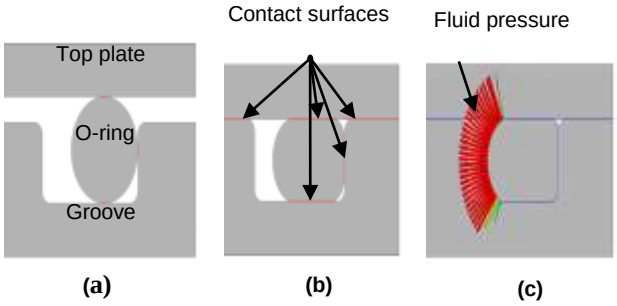

Figure 3 - (a) Mounting the O-ring in a groove. (b) Compression of the O-ring. (c) Application of fluid pressure

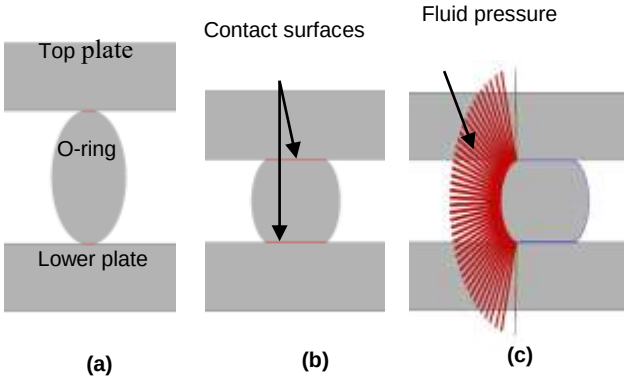

Figure 4 - (a) Mounting the O-ring between two plates. (b) Compression of the O-ring. (c) Application of fluid pressure

3. Conventional Analytical Theory

This part summarizes the set of equations that give the distribution of the contact pressure, the maximum value of this contact pressure, and the length of the contact that characterizes the joint-plate contact area. The joint-plate contact has been treated by Lindley [2] by adapting the classical theory of Hertz. This researcher developed a simple equation that expresses the compressive load, F, as a function of the compression ratio of the joint, C, according to the equation.

$$F = \pi d_0 d_2 E^* (1.25C^{\frac{3}{2}} + 50C^6) \quad (1)$$

The compression ratio of the joint, C, is determined as a function of the crushing values, e, and the diameter of the joint cross-section d_2. It is expressed as follows:

$$C = e/d_2$$

The contact width, l, the maximum value of contact pressure, P_0 are given by equations (2) and (3).

$$l = 2\sqrt{\frac{4PR^*}{\pi E^*}} \quad (2)$$

$$p_0 = \frac{4F}{\pi^2 d_0 l} \quad (3)$$

With R^* the relative radius of curvature and E^* the equivalent modulus of elasticity.

The relative radius of curvature, R^*, is determined according to the type of contact. Thus in the case of the plane-cylinder contact adopted by Lindley we have

$$R^* = \frac{d_2}{2} \quad (4)$$

The equivalent modulus of elasticity is given by equation (5).

$$E^* = \frac{E_1}{1-\nu_1^2} \quad (5)$$

The distribution of the contact pressure as a function of the radial position on the joint is given by equation (6).

$$p(x) = p_0\sqrt{1-\left(\frac{2x}{l}\right)^2} \quad (6)$$

4. Results and Discussions

To verify the finite element models developed in this chapter, we have made comparisons with the theoretical results presented by Lindley [2] and the experimental results of Kim et al. [32]. A first simulation is performed

considering a zero fluid pressure and a zero friction coefficient. results were obtained with the FE model presented in Figure 4 and compared to the results of the values of equation (1) developed by Lindley [2] and those published by Kim et al. [32]. We note a very good agreement between the results obtained by the analytical model and the results of the FE model. However, there is a significant discrepancy between the two models and the experimental test of Kim et al. for compression ratios greater than 15%. This difference may be due to the geometrical and physical data considered by the authors when establishing their model.

Both the analytical and numerical models are used to determine the contact width values and contact pressure distribution profiles when a clamping load is applied. Figure 6 shows a comparison between the contact width values given by equation (2) and the FE model results shown in Figure 4. The FE model results are the average value of the last nodes in contact and the first nodes not in contact. The difference between the numerical and analytical curves is at most 5% at a clamping force of 350 N, which corresponds to a compression ratio of 27% in this case. It is important to recall that Lindley [2] describes the relationship of contact-displacement force, contact width, and contact pressure as a function of O-ring radial position for a maximum O-ring compression ratio of 25%.

Figure 7 shows the contact pressure distributions on the surface A1 defined in Figure 1 for four values of clamping force. This figure also shows a comparison between the analytical and numerical models. The contact pressure profiles have a parabolic shape that confirms the Hertzian shape. The comparison between the values of the analytical model and the results of the FE analysis indicates that the maximum contact pressure increases as the clamping force increases and the difference between the two models do not exceed 4%. From these remarks, we can confirm that there is a good agreement between the two approaches, analytical and FE, when the only load applied is the clamping force.

The effect of friction was considered from the finite element simulation of assemblies 1 and 2 shown in Figures 3 and 4. The axial and radial deformations of the O-ring as a function of clamping force and fluid pressure are obtained for f values of 0, 0.1, and 0.2 (Figure 8). This figure shows the importance of the location of this type of seal in a groove. For a clamping force of 700 N and a fluid pressure of 0.75 MPa, the increase in the friction coefficient considerably reduces the axial and radial deformation of the seal. Indeed, for friction coefficients 0, 0.1 and 0.2. The elongation decreases respectively from 66.5, 19.5 to 2.7%. Regarding the compression ratio, it decreases respectively from 48.9, 37.3 to 30.9. In conclusion, the deformation of the joint as a function of the clamping load and the pressure of the fluid depends strongly on the value of the friction coefficient. Figure 9 shows the variation of the maximum contact pressure, at the surfaces B1, B2 and B3 defined in Figure 3, for two values of friction coefficients 0.05 and 0.2, according to the pressure of the confined fluid. It can be seen that the influence of the friction coefficient on the contact pressure is negligible. Furthermore, by studying Figure 10, the increase of the friction coefficient can decrease the maximum value of the von Mises stress inside the O-ring installed in a groove for high fluid pressures and the opposite for low fluid pressures. Given the particularity of the material characteristics of the O-ring, a parametric study to understand the influence of Young's modulus E becomes necessary. Several simulations were performed, for the same geometry of the FE model presented in Figure 3, for Young's modulus ranging from 6.96 MPa to 17.3 MPa. The numerical calculations were carried out with a coefficient of friction of 0.2. Figure 11 shows the evolution of the compression ratio C, obtained for three values of Young's modulus E, weighting the two phases of deformation of the seal: clamping phase F, and pressurization phase P. The results delivered by this figure serve as a basis for determining the influence of these three parameters on the compression ratio of the seal in the throat. It is obvious that the compression ratio increases with increased clamping force and decreases with increasing fluid pressure. As can be seen in the same figure, the compression ratio is proportional to Young's modulus. It can be observed in the clamping phase that, the stiffer the seal material, the lower the compression ratio will be. On the other hand, when the fluid pressure is applied and increases further, the value of the compression ratio decreases. It is also observed that the curves corresponding to the three values of Young's modulus are inverted when the fluid pressure exceeds 4.75 MPa. Figure 12 shows the contact pressure distribution curves at the contact surfaces B1, B2 and B3 defined in Figure 1, for a compression ratio of 20% and a fluid pressure of 5 MPa. The simulations are performed for several values of E. The curves in this figure confirm that the stresses are proportional to the moduli of elasticity for the same deformation. Thus, when the joint stiffness is greater, the contact pressure is greater. Figure 13 shows the variation of the maximum value of Von Mises stress inside the seal for three values of E as a function of fluid pressure for a compression ratio of 20%. Regardless of the value of E, the maximum Von Mises stress increases with increasing rates as the fluid pressure increases. We note that the difference between the three seal hardnesses shows a high value for pressures below 5.5 MPa and remains relatively low for fluid pressures above this value. This result does not surprise us. Indeed, whatever the value of E, when the fluid pressure is applied and its value increases, the zone where the stress is maximum moves towards the outside of the joint to the side of the extrusion gap. Lastly, it is worth mentioning that the compression ratio as a function of clamping force - Numerical/ analytical/ experimental comparison is presented in Figure 5.

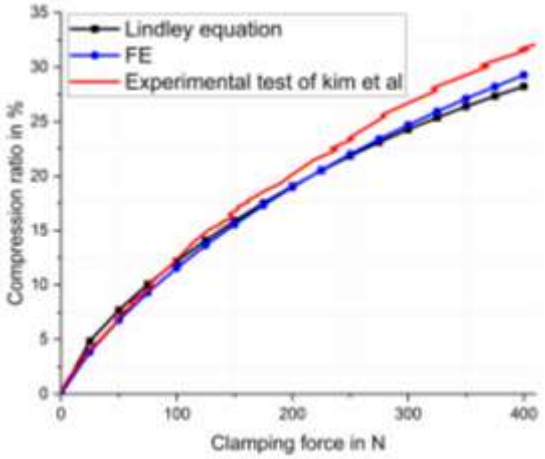

Figure 5 - Compression ratio as a function of clamping force - Numerical/ analytical/ experimental comparison

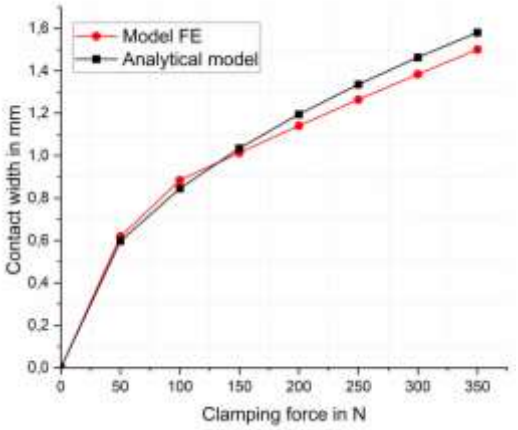

Figure 6 - Contact width versus clamping force - numerical/analytical comparison

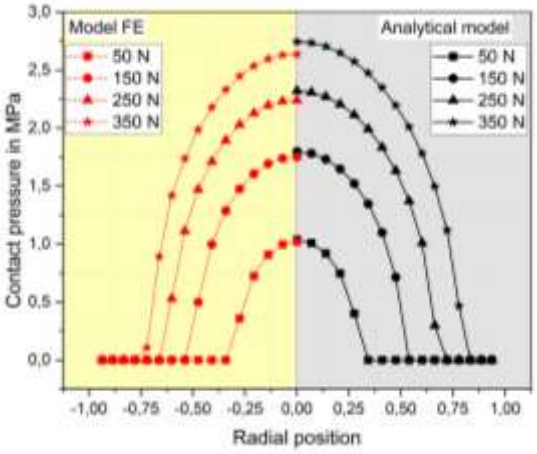

Figure 7 - Distribution of contact pressure as a function of clamping force - numerical/analytical comparison

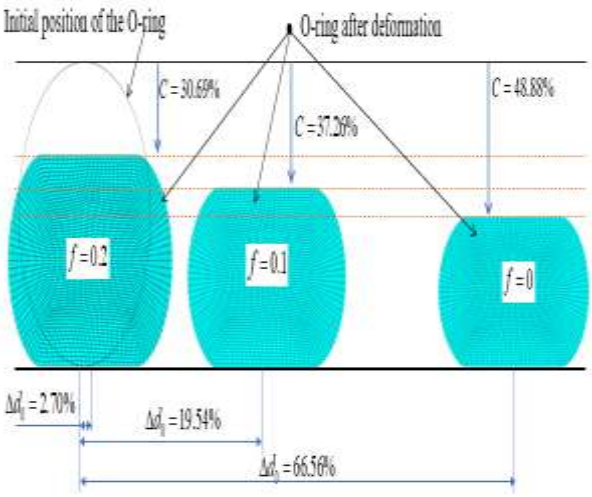

Figure 8 - The influence of the friction coefficient on the deformation of the O-ring

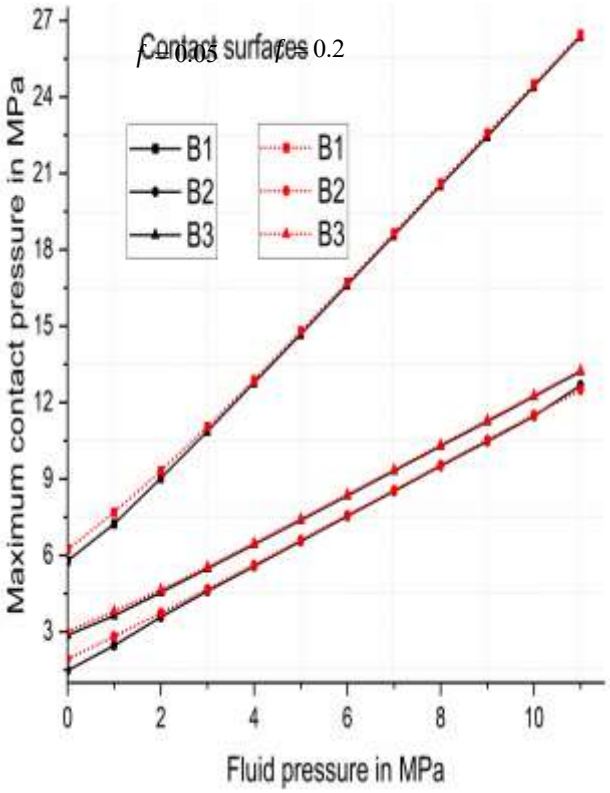

Figure 9 - The influence of the friction coefficient on the maximum contact pressure

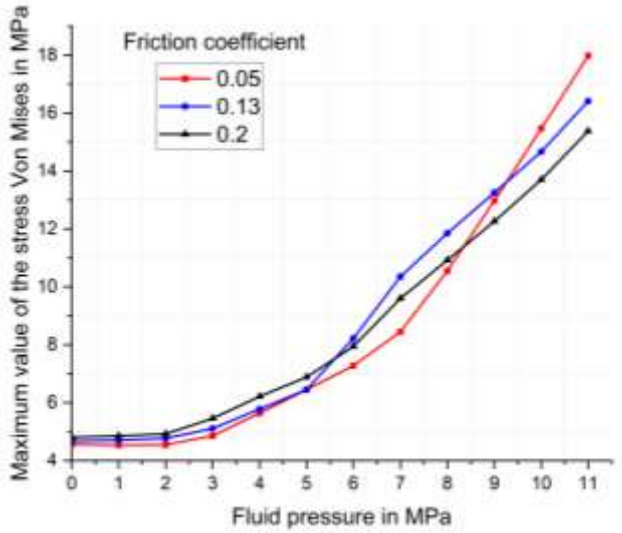

Figure 10 - The influence of the friction coefficient on the maximum value of the Von Mises stress

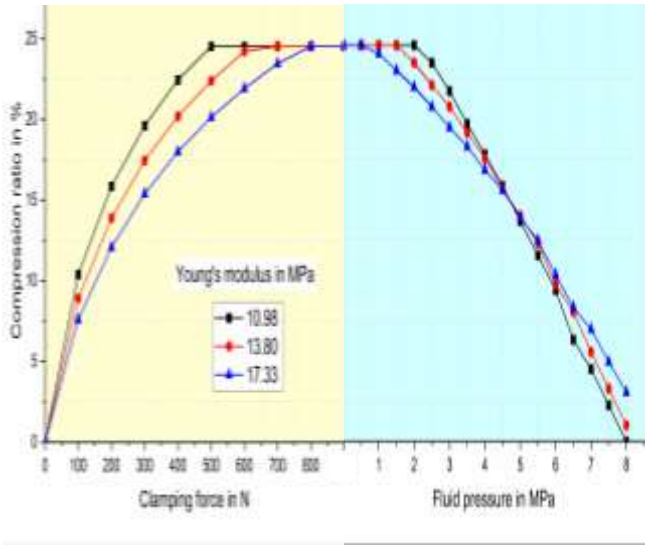

Figure 11 - Variation of compression ratio with the variation of clamping force and fluid pressure

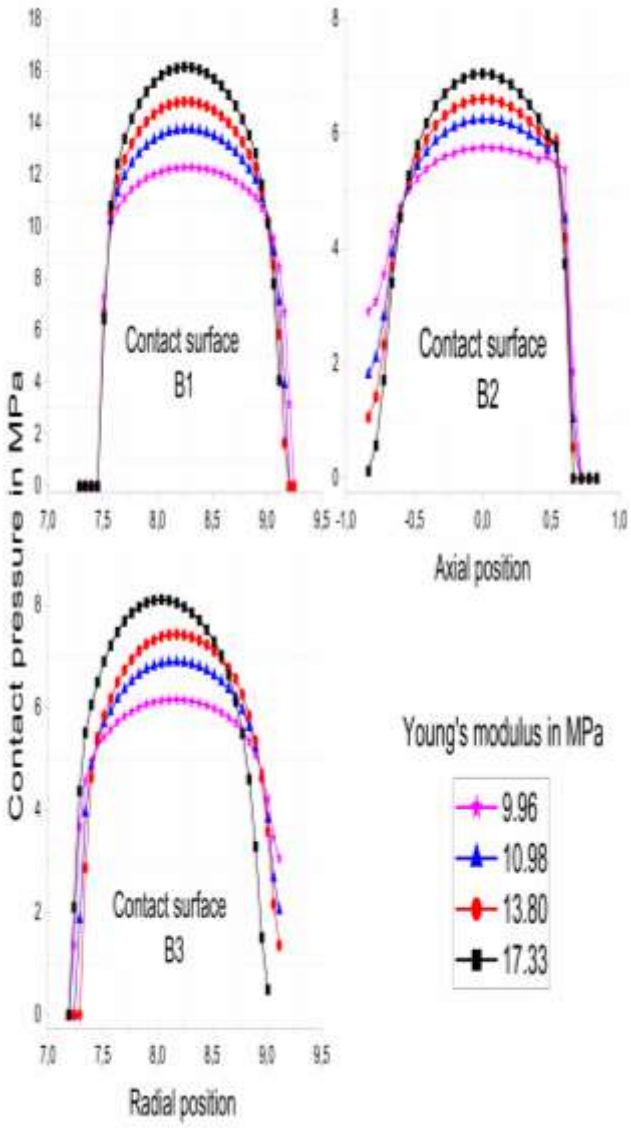

Figure 12 - Influence of Young's modulus on the contact pressure distribution for a compression ratio of 20% and a fluid pressure of 5 MPa

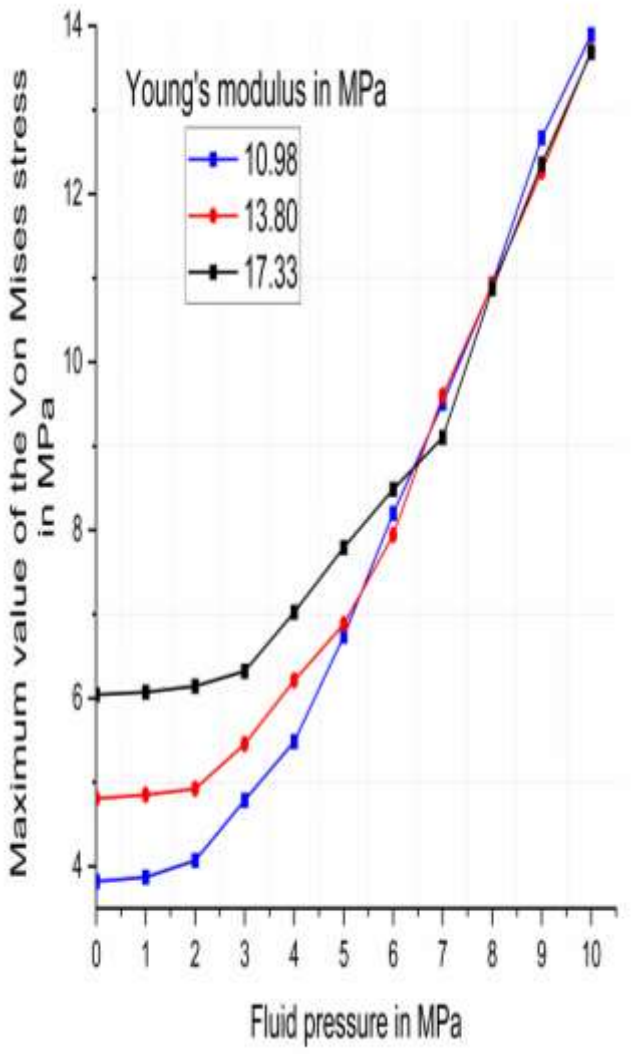

Figure 13 - influence of Young's modulus on the maximum value of the Von Mises stress for a compression ratio of 20%

5. Conclusions

This work is devoted to the study of the mechanical and leakage behavior of pressurized assemblies equipped with an O-ring which is placed in a groove and between two plates. The material behavior of the O-ring has been described by the Mooney Rivlin behavior law. The finite element model of the gasket was carried out with axisymmetric elements under the assumption of large displacements and large deformations using the commercial software (ANSYS).

The combined effect of clamping load and fluid pressure has been analyzed for both assemblies. The numerical results obtained are compared with the experimental results published by Kim et al. [20] and theoretically based on the classical Hertz theory. The comparison is made only on the clamping force, contact width, and contact pressure. They show agreement and confirm the classical form of the contact pressure distribution.

This study shows that the use of a groove to ensure the assembly of elastomer O-rings is important in pressurized installations. On the other hand, under the same loading conditions, the reliability of the O-ring is strongly dependent on three parameters: compression ratio of the O-ring, its hardness, and the friction coefficient.

References

[1] N. A. Christensen, "Packing." Google Patents, 21-Nov-1939.

[2] P. B. Lindley, "Compression characteristics of laterally-unrestrained rubber O-rings," *J. Inst. Rubber Ind*, vol. 1, no. 4, pp. 209–213, 1967.

[3] S. P. Timošenko and J. N. Goodier, *Theory of elasticity*. McGraw-Hill, 1951.

[4] E. Dragoni and A. Strozzi, "Analysis of an Unpressurized, Laterally Restrained, Elastomerio O-Ring Seal," *Journal of Tribology*, vol. 110, no. 2, pp. 193–200, 1988.

[5] A. Karaszkiewicz, "Geometry and Contact Pressure of an O-Ring Mounted in a Seal Groove," *Industrial and Engineering Chemistry Research*, vol. 29, no. 10, pp. 2134–2137, 1990.

[6] A. F. George, A. Strozzi, and J. I. Rich, "Stress fields in a compressed unconstrained elastomeric O-ring seal and a comparison of computer predictions and experimental results," *Tribology International*, vol. 20, no. 5, pp. 237–247, 1987.

[7] R. Eshel, "Prediction of extrusion failures of o-ring seals," *ASLE Transactions*, vol. 27, no. 4, pp. 332–340, 1984.

[8] K. Yokoyama, M. Okazaki, and T. Komito, "Effect of contact pressure and thermal degradation on the sealability of O-ring," vol. 19, pp. 123–128, 1998.

[9] J. Nam, J. Hawong, S. Han, and S. Park, "Contact stress of O-ring under uniform squeeze rate by photoelastic experimental hybrid method," *Journal of Mechanical Science and Technology*, vol. 22, no. 12, pp. 2337–2349, 2008.

[10] J. H. Nam, J. S. Hawong, K. H. Kim, Liu-Yi, O. S. Kwon, and S. H. Park, "A study on the development of a loading device using a photoelastic stress freezing method for the analysis of o-ring stress," *Journal of Mechanical Science and Technology*, vol. 24, no. 3, pp. 693–701, 2010.

[11] J. H. Nam, J. S. Hawong, D. C. Shin, and B. R. Mose, "A study on the behaviors and stresses of O-ring under uniform squeeze rates and internal pressure by transparent type photoelastic experiment," *Journal of Mechanical Science and Technology*, vol. 25, no. 9, pp. 2427–2438, 2011.

[12] Y. Sang, X. Wang, W. Sun, and P. Liu, "Numerical and experimental study on the friction of O ring for hydraulic seals," *Australian Journal of Mechanical Engineering*, vol. 00, no. 00, pp. 1–13, 2019.

[13] N. Wang, S. Pang, C. Ye, T. Fan, and S. B. Choi, "The friction and wear mechanism of O-rings in magnetorheological damper: Numerical and experimental study," *Tribology International*, vol. 157, May 2021.

[14] S. Stupkiewicz and A. Marciniszyn, "Elastohydrodynamic lubrication and finite configuration changes in reciprocating elastomeric seals," *Tribology International*, vol. 42, no. 5, pp. 615–627, 2009.

[15] C. J. Han and J. Zhang, "Finite element analysis and optimization of rectangle rubber seal," *China Rubber Industry*, vol. 60, no. 2, pp. 98–103, 2013.

[16] B. Yang and R. F. Salant, "Elastohydrodynamic lubrication simulation of O-ring and U-cup hydraulic seals," vol. 225, pp. 603–610, 2010.

[17] M. El Gadari and M. Hajjam, "Effect of the Grooved Rod on the Friction Force of U-Cup Hydraulic Rod Seal with Rough Lip," *Tribology Transactions*, vol. 61, no. 4, pp. 661–670, 2018.

[18] Z. Zhang, D. Wu, H. Pang, Y. Liu, W. Wei, and R. Li, "Extrusion-occlusion dynamic failure analysis of O-ring based on floating bush of water hydraulic pump," *Engineering Failure Analysis*, vol. 109, p. 104358, 2020.

[19] W. Song and W. Cui, "Finite element analysis of large-sized O-rings used in deep-ocean pressure chambers," *Advances in Mechanical Engineering*, vol. 13, no. 8, p. 168781402110406, 2021.

[20] M. Diany and H. Aissaoui, "Analytical and Finite Element Analysis for Short term O-ring Relaxation," *Applied Mechanics and Materials*, vol. 61, no. 6, pp. 478–482, 2011.

[21] H. Aissaoui, M. Diany, and J. Azouz, "Numerical simulation of radial and axial compressed eleastomeric o-ring relaxation," *Global Journal of Researches in Engineering Mechanical and Mechanics Engineering*, vol. 12, no. 4, 2012.

[22] E. Bahloul, M. Diany, H. Aissaoui, E. Boudaia, J. Azouz, and M. Mabrouki, "Finite element analysis of the O-ring behavior used in static sealing assembly," pp. 106–108, 2019.

[23] E. M. EL Bahloul, M. Diany, H. Aissaoui, E. Boudaia, and M. Mabrouki, "Finite Element Analysis of O-ring Performance Reinforced by a Metallic Core," *International Journal of Fluid Power*, vol. 23, pp. 237–252, 2022.

[24] E. El Bahloul, M. Diany, H. Aissaoui, E. Boudaia, and M. Mabrouki, "Analysis of the Sealing Performance of a Concave O-Ring Groove," *International Review of Mechanical Engineering*, vol. 15, no. October, pp. 530–537, 2021.

[25] ANSYS, ANSYS Standard Manual, Version 19.2

[26] ANSYS Inc., "ANSYS Mechanical APDL Technology Demonstration Guide," *Knowledge Creation Diffusion Utilization*, vol. 3304, no. October, pp. 724–746, 2012.

[27] B. Omnès, *Comportement mécanique des joints toriques*. Centre technique des industries mécaniques., 2016.

[28] J. Mackerle, "Rubber and rubber-like materials, finite-element analyses and simulations, an addendum: A bibliography (1997-2003)," *Modelling and Simulation in Materials Science and Engineering*, vol. 12, no. 5, pp. 1031–1053, 2004.

[29] L. Mullins, *Engineering With Rubber.*, vol. 17, no. 12. 1987.

[30] H. K. Müller and B. S. Nau, *Fluid sealing technology: principles and applications*. Routledge, 2019.

[31] ISO 3601, Fluid power systems – O-rings. Part 1: Inside diameters, cross-sections, tolerances, and designation codes. Part 2: Housing dimensions for general applications. Part 3: Quality acceptance criteria. Part 4: Anti-extrusion rings (back-up rings). Part 5: Suitability of elastomeric materials for industrial applications.

[32] H. Kim, S. Park, H. Lee, D. Kim, and Y. Lee, "Approximation of contact stress for a compressed and laterally one side restrained O-ring," vol. 14, pp. 1680–1692, 2007.

Contribution of Individual Authors to the Creation of a Scientific Article (Ghostwriting Policy)

The author(s) contributed in the present research, at all stages from the formulation of the problem to the final findings and solution.

Sources of Funding for Research Presented in a Scientific Article or Scientific Article Itself

No funding was received for conducting this study.

Conflict of Interest

The author(s) declare no potential conflicts of interest concerning the research, authorship, or publication of this article.